Electronic Journal of Differential Equations, Vol. 2015 (2015), No. 104, pp. 1–19.
ISSN: 1072-6691. URL: http://ejde.math.txstate.edu or http://ejde.math.unt.edu
ftp ejde.math.txstate.edu

THREE MODELS FOR RECTILINEAR PARTICLE MOTION WITH THE BASSET HISTORY FORCE

SHUJING XU, ALI NADIM

Abstract. We consider three model problems that describe rectilinear particle motion in a viscous fluid under the influence of the Basset history force. These problems consist of sedimentation starting from rest, impulsive motion in a quiescent fluid, and oscillatory sliding motion. The equations of motion are integro-differential equations with a weakly singular kernel. We derive analytical solutions to all three problems using Laplace transforms and discuss the mathematical relation between the sedimentation and impulsive start problems. We also compare several numerical schemes for solving the integro-differential equations and benchmark them against the analytical results.

1. Introduction

The dynamics of a solid particle moving in a flowing liquid or gas is of great interest in the field of fluid dynamics for it has broad application in physics, biology, multiphase flow, etc. In the present paper, three fundamental one-dimensional motions are examined in the presence of the history force: sedimentation of a particle in a quiescent fluid in which the particle is released from rest, impulsive motion where the particle is given an initial velocity or impulse and subsequently relaxes under the influence of viscosity, and an oscillatory sliding motion where a fluid-filled cartridge containing the particle undergoes a back and forth motion.

For a small, spherical, non-deformable particle moving in an unbounded flow domain, the equation of motion is given by [18]

$$\begin{aligned} m_p\frac{d\mathbf{V}}{dt} &= m_f\frac{D\mathbf{u}}{Dt} - \frac{1}{2}m_f\Big(\frac{d\mathbf{V}}{dt} - \frac{D\mathbf{u}}{Dt}\Big) - 6\pi\mu a(\mathbf{V}-\mathbf{u}) \\ &\quad + (m_p - m_f)\mathbf{g} - 6a^2\sqrt{\pi\mu\rho_f}\int_{-\infty}^{t}\frac{1}{\sqrt{t-\tau}}\Big(\frac{d\mathbf{V}}{d\tau} - \frac{D\mathbf{u}}{D\tau}\Big)d\tau\,, \end{aligned} \tag{1.1}$$

where m_p is the particle mass; m_f the displaced fluid mass; $\mathbf{V}(t)$ the particle velocity; $\mathbf{u}(\mathbf{x},t)$ the fluid velocity field; a the radius of the particle; μ the dynamic viscosity of the fluid, and ρ_f its density. Two time derivatives, D/Dt and d/dt, are used to measure the rate-of-change of fluid velocity seen by an observer moving along with the fluid and the particle, respectively.

2010 *Mathematics Subject Classification.* 76T20, 45J05, 65L05.
Key words and phrases. Particle motion; history force; integro-differential equations; Laplace transforms; numerical methods; multiphase flow.

Submitted November 7, 2014. Published April 21, 2015.

In addition to the pressure stress, added mass, viscous drag, and gravity as shown on the right-hand side of (1.1), a history-type force depending on the entire history of the motion is also known to play a role (the last term in the equation). This Boussinesq-Basset force accounts for the temporal delay in boundary layer development with changing relative velocity of bodies moving through a fluid. This unsteady force acting on a particle submerged in a fluid was first investigated by Joseph Valentin Boussinesq [5] and Alfred Barnard Basset [2]. It is also known simply as the history force, a combination of both viscous and inertial contributions to the force in that it depends on both the viscosity and density of the fluid and the acceleration of the particle [16]. For the motion of rigid spheres in a viscous fluid, the regimes where the history force might be negligible or is significant have been investigated. Parameters that determine the significance of the history term include velocity fluctuations in time, contrasting fluid-to-particle density ratio, and the particle Reynolds number [8, 9, 14, 15, 16, 17, 19, 21, 23, 25, 28].

The history term turns the equation of motion into an integro-differential equation implicit in the dependent variable $\mathbf{V}(t)$ for it also appears inside the integrand and makes it challenging to solve for the motion. As its name suggests, the history force involves an integral based on the entire history of the motion up to the present time. For practical reasons, the starting point in time is usually set as 0 instead of $-\infty$, under the assumption that there is no prehistory before time 0. Even with such simplification, for each time step, it is still necessary to make use of all former values, which increases both the computational time and the memory requirements. Another challenge lies in the fact that the integrand has a singularity near its upper limit, which prevents one from using traditional methods for performing the numerical quadrature. Overcoming these numerical challenges is one aspect of the present work.

For certain problems involving the history force, exact analytical solutions can be obtained. For these, Laplace transforms turn out to be the most fruitful approach for obtaining the solutions in the time domain: e.g., for a sphere undergoing free fall in a still, viscous fluid [6], a sphere in creeping flow [20], and an isolated denser particle dropped in the core of a vertical vortex [7]. Lovalenti and Brady [16] pointed out one of the limitations of using Laplace transforms (in time) when dealing with time-dependent coefficients. For a particle suspended in homogeneous turbulence responding to the random velocity field, Mei et al [19] resorted to Fourier transforms to obtain the analytical solution in the frequency domain. [30] evaluated the trajectories of an accelerating spherical drop at low Reynolds number by transforming the result from the Fourier-transform domain. Other analytical approaches include the use of Abel's theorem to investigate linear models for a sphere falling through a Newtonian fluid [3]; manipulating the operators, for example, writing the integral

$$I(f(t)) = \frac{1}{\sqrt{\pi}} \int_0^t \frac{f(x)}{\sqrt{t-x}} dx = \frac{2}{\sqrt{\pi}} \int_0^{\sqrt{t}} f(t-x^2) dx$$

when the Cauchy problem is involved [26, 27], and the use of the Γ function similarly in [31]. Coimbra et al [11] generalized how to obtain the solution of the particle equation analytically for unsteady Stokes flows. First, they applied a fractional-differential operator to the first-order integro-differential equation of motion in order

to transform the original equation into a second-order non-homogeneous equation, and then they solved this last equation by the method of variation of parameters.

On the numerical side, Brush et al [6] proposed a trapezoidal-based method under the assumption that on a small enough time interval, the derivatives in the integrand could be roughly regarded as a constant and be brought outside the integral sign, with the rest of the integrand evaluated analytically. Taylor expansions were employed in [12, 13] to improve the accuracy; however, this came at a cost of much longer computational time. Bombardelli et al [4] considered the integral as a fractional derivative that could be approximated by a summation series which had a first order temporal accuracy. An approximation based on exponential functions was described in [24] and shown to have second-order accuracy; however, the choice of exponential functions varies from one situation to the next.

In this work, we focus on three model problems whose exact solutions can be obtained analytically. Among these, the exact solution for particle trajectories in an oscillatory sliding motion is new. We also use these exact solutions to benchmark some numerical schemes for solving such problems. The rest of the present paper is structured as follows. Section 2 introduces two numerical treatments for the problematic history integral in detail. This is followed in Section 3 with the three physical problems involving one-dimensional motion: sedimentation, impulsive motion, and oscillatory sliding motion. For each problem, the scaled equation of motion is presented, along with its analytical solution which is used to benchmark the corresponding numerical methods. Selected numerical methods from the existing literature are also applied to the same problems by way of comparison. Section 4 provides our summary and conclusions.

2. Numerical approximation of the singular integrals

For both methods that will be presented, the uniform time step is denoted by Δt in the temporal discretization and the initial time t_1 is taken to be 0. Thus, any given time t_n is given by $t_n = (n-1)\Delta t$, and the discrete analog of any function $f(t)$ at t_n is denoted by $f(t_n)$ or simply f_n.

2.1. Forward difference hybrid.

The first method introduced is a combination of trapezoidal rule and integration by parts carried out in two stages. It can be viewed as a refined version of the trapezoidal-based method proposed by Brush in which it was assumed that the integrand on a small interval is a constant. To introduce this two-stage scheme, let us start with rewriting the integral history term in the form

$$I(t) = \int_0^t \frac{f(\tau)}{\sqrt{t-\tau}}\, d\tau\,. \tag{2.1}$$

In (1.1), $f \equiv d\mathbf{V}/d\tau - D\mathbf{u}/D\tau$, and is differentiable everywhere. When τ gets close to the upper limit t, the singularity prevents us from applying the trapezoidal rule directly. An intuitive idea is to isolate the troublemaker, i.e., break up the integral into two parts, one containing the singularity on a very small interval (as $\Delta t \to 0$) and the other being free of singularity. That is, at any given time t_n, the integral can be evaluated by

$$I(t_n) = \int_0^{t_n} \frac{f(\tau)}{\sqrt{t_n-\tau}} d\tau = \int_0^{t_{n-1}} \frac{f(\tau)}{\sqrt{t_n-\tau}} d\tau + \int_{t_{n-1}}^{t_n} \frac{f(\tau)}{\sqrt{t_n-\tau}} d\tau\,.$$

Apply the trapezoidal rule to the first term on the right-hand side. Integrate the second term by parts on the small interval $[t_{n-1}, t_n]$, then apply the trapezoidal rule. The derivative of the function at t_{n-1} is generated as a result of the process. To evaluate its value, there are multiple options, for instance, forward, backward and central differences. We have tested the above-mentioned finite difference methods on the cases where exact solutions are available; they appear to have the same level of accuracy and computational speed; however, forward difference is our choice as it is slightly more accurate. Combining the two parts, we obtain the expression to approximate the integral

$$I_n = \Delta t \sum_{i=2}^{n-1} \frac{f_i}{\sqrt{t_n - t_i}} + \frac{\Delta t}{2}\Big(\frac{f_1}{\sqrt{t_n - t_1}} - \frac{f_{n-1}}{\sqrt{t_n - t_{n-1}}}\Big) + \sqrt{\Delta t}\,(f_{n-1} + f_n)\,. \quad (2.2)$$

The scheme introduced here is a combination of two techniques, during which forward finite differencing is applied; we will thus refer to it as the FD Hybrid method in this paper. In Nevskii and Osiptsov's study of the effects of unsteady and history forces in the gravity convection of suspensions [22], a similar scheme has been mentioned.

2.2. **Predictor corrector method.** Noticing that often the numerator of the integrand involves time-derivatives of various terms, instead of what has been shown in (2.1), the integral is rewritten in the following way:

$$I(t) = \int_0^t \frac{\dot f(\tau)}{\sqrt{t-\tau}}\, d\tau\,. \quad (2.3)$$

On each subinterval $[t_{j-1}, t_j]$, $j = 2, \dots, n$, approximate $\dot f(\tau)$ by forward difference at t_{j-1} (which may also be regarded as a central difference approximation at the midpoint of the interval); then the rest of the integral can be integrated analytically. When applied to the entire interval, a weighted sum is obtained to approximate the integral, namely,

$$I_n = \frac{2}{\Delta t} \sum_{j=2}^{n} \big[\sqrt{t_n - t_{j-1}} - \sqrt{t_n - t_j}\,\big]\,(f_j - f_{j-1}). \quad (2.4)$$

In the process of evaluating the time-dependent function at the next step, a predictor-corrector scheme based on this formula for evaluating the integral can then be applied effectively to improve accuracy. In combination with the time-stepping formula, this scheme will be referred to as the PC Method. This turns out to be similar to the approach of discretizing the history integral in [23], further developed by Alexander [1].

3. Physical problems in one dimension

To test the above schemes, we apply both to various physical problems for which exact analytical solutions are attainable so that we can compare the numerical results against the exact solutions thereby validating the methods. By way of comparison, selected numerical methods from the existing literature are also applied to the same problems.

3.1. **Sedimentation.** The first problem we consider is sedimentation under gravity. For a sphere initially released from rest in an infinite stagnant fluid, upon nondimensionalizing the particle's velocity with the steady Stokes settling velocity: $(2a^2g\Delta\rho)/(9\mu)$, and scaling time with the viscous diffusion time: a^2/ν (most physical parameters were introduced in Section 1; additionally $\nu = \mu/\rho_f$ is the kinematic viscosity and $\Delta\rho$ is the difference between the densities of the particle and fluid), the dimensionless equation of motion is given by [10]

$$\begin{gathered}\frac{1}{B}\frac{dW}{dt} = 1 - W - \frac{1}{\sqrt{\pi}}\int_0^t \frac{\dot{W}(\tau)}{\sqrt{t-\tau}}d\tau,\\ W(0) = 0, \quad \frac{dW}{dt}(0) = B\,,\end{gathered} \tag{3.1}$$

where $W(t)$ is the ratio of the instantaneous velocity to the steady settling velocity in Stokes flow, and B is the dimensionless acceleration, dW/dt, at $t = 0$, which depends solely on the density ratio $\gamma = \rho_p/\rho_f$, specifically, $B = 9/(2\gamma + 1)$. Note that the second initial condition on dW/dt can be inferred from the differential equation itself by evaluating both sides at $t = 0$ and using the first initial condition on W. Thus, strictly speaking, it is not needed. Depending on whether the density ratio γ is less than, equal to, or greater than the critical value $\gamma_c = \frac{5}{8}$ (corresponding to $B_c = 4$), (3.1) has the analytical solution

$$W(t) = \begin{cases} 1 - \dfrac{a}{a-b}\exp(b^2t)\operatorname{Erfc}(b\sqrt{t}) - \dfrac{b}{b-a}\exp(a^2t)\operatorname{Erfc}(a\sqrt{t}) & B > 4,\\ 1 + (8t-1)\exp(4t)\operatorname{Erfc}(2\sqrt{t}) - 4\sqrt{t/\pi} & B = 4,\\ 1 - \Re\{W[(Y+iX)\sqrt{t}]\} - \dfrac{X}{Y}\Im\{W[(Y+iX)\sqrt{t}]\} & B < 4, \end{cases}$$

where $a = \frac{B}{2}(1 + \sqrt{1 - 4/B})$, $b = \frac{B}{2}(1 - \sqrt{1 - 4/B})$, $X = \frac{B}{2}$, $Y = \frac{B}{2}\sqrt{4/B - 1}$ and $W(Z)$ is the complex error function $W(Z) = \exp(-Z^2)\big(1 + \frac{2i}{\sqrt{\pi}}\int_0^Z \exp(\xi^2)\,d\xi\big)$, with $\Re$ and $\Im$ referring to the real and imaginary parts. Erfc is the complementary error function defined by $\operatorname{Erfc}(z) \equiv 1 - \operatorname{Erf}(z) = \frac{2}{\sqrt{\pi}}\int_z^\infty \exp(-t^2)dt$. The expression for $B < 4$ is also equivalent to the real part of the expression given for $B > 4$. Both reduce to the middle expression when B approaches 4.

3.1.1. *Numerical solution.* To approximate $W(t)$ at the $(n+1)$-st time step, forward differencing is applied to the derivative in (3.1) resulting in the update equation

$$w_{n+1} = B\Delta t + (1 - B\Delta t)w_n - \frac{B\Delta t}{\sqrt{\pi}}\,I_n\,, \tag{3.2}$$

where w_n is the numerical solution at t_n and I_n is the numerical approximation of the integral $\int_0^t \frac{\dot{W}(\tau)}{\sqrt{t-\tau}}d\tau$ at the n-th time step. We then apply (2.2) and (2.4) to the integral and obtain trajectories accordingly.

3.1.2. *Implementation of FD Hybrid and PC methods.* We now demonstrate how to implement the two methods in full detail for the 1-D sedimentation problem. Detailed descriptions for the other problems will not be given, since they are quite similar to this one.

FD Hybrid: Apply (2.2) to I_n in (3.2). Notice that (2.2) requires $n \geq 3$, that is, if we denote the discretized velocity as the sequence w_i $(i = 1, 2, \dots)$, we need to know w_1, w_2, w_3 before we can apply the update equation. From the initial conditions, it

is natural to let $w_1 = 0$, $w_2 = B\Delta t + w_1$ by first-order forward finite differencing, and $w_3 = -2\big(B\Delta t + \frac{3}{2}w_1 - 2w_2\big)$ by the second-order forward finite differencing for the first derivative. Effectively, this ends up approximating the solution as a straight line along the first three time nodes. Then I_3 is given by

$$\begin{aligned} I_3 &= \Delta t\frac{\dot{w}_2}{\sqrt{t_3 - t_2}} + \frac{\Delta t}{2}\Big(\frac{\dot{w}_1}{\sqrt{t_3 - t_1}} - \frac{\dot{w}_2}{\sqrt{t_3 - t_2}}\Big) + \sqrt{\Delta t}\,(\dot{w}_2 + \dot{w}_3) \\ &= \frac{w_3 - w_2}{\sqrt{\Delta t}} + \frac{1}{2}\Big(B\sqrt{\frac{\Delta t}{2}} - \frac{w_3 - w_2}{\sqrt{\Delta t}}\Big) + 2\frac{w_3 - w_2}{\sqrt{\Delta t}} \\ &= \frac{B\sqrt{\Delta t}}{2\sqrt{2}} + \frac{3(w_3 - w_2)}{2\sqrt{\Delta t}}\,. \end{aligned}$$

Here the derivatives are approximated by forward difference, except that we use backward on the term $\dot{w}_3$. In general, for $n \geq 3$, the updating expression for the memory integral is

$$\begin{aligned} I_n &= \Delta t\sum_{i=2}^{n-1}\frac{\dot{w}_i}{\sqrt{t_n - t_i}} + \frac{\Delta t}{2}\Big(\frac{\dot{w}_1}{\sqrt{t_n - t_1}} - \frac{\dot{w}_{n-1}}{\sqrt{t_n - t_{n-1}}}\Big) + \sqrt{\Delta t}\,(\dot{w}_{n-1} + \dot{w}_n) \\ &= \sum_{i=2}^{n-1}\frac{w_{i+1} - w_i}{t_n - t_i} + \frac{1}{2}\Big(\frac{B\Delta t}{\sqrt{t_n - t_1}} - \frac{w_n - w_{n-1}}{\sqrt{\Delta t}}\Big) + \frac{2(w_n - w_{n-1})}{\sqrt{\Delta t}}\,, \end{aligned}$$

which can be substituted into (3.2) to complete the implementation.

PC method: Apply (2.4) to I_n in (3.2). The PC Method requires only two initial points to get started as suggested in (2.4), that is, $w_1 = 0$ and $w_2 = B\Delta t + w_1$. Thus after substitution and simplification,

$$I_2 = \frac{2}{\sqrt{\Delta t}}\,(w_2 - w_1).$$

In general for $n \geq 2$, the update expression to estimate the memory integral in 1-D sedimentation is given by

$$I_n = \frac{2}{\Delta t}\sum_{j=2}^{n}\big[\sqrt{t_n - t_{j-1}} - \sqrt{t_n - t_j}\big]\,(w_j - w_{j-1}). \tag{3.3}$$

However, in the PC Method, two evaluations of the integral are required for each time step. Suppose we have obtained the sequence $w_1, w_2, \ldots, w_n$. To approximate w_{n+1}, the first step is to obtain the approximation for the history integral I_n using (3.3). In the "predictor" step, we continue by obtaining an approximation to w_{n+1} by (3.2); let us call this w^*_{n+1}. We then use the resulting length $(n+1)$ sequence of w_i to evaluate the integral again, denoted as I^*_{n+1}. The "predictor" step then produces the final desired w_{n+1} using

$$w_{n+1} = B\Delta t + (1 - B\Delta t)\frac{w_n + w^*_{n+1}}{2} - \frac{B\Delta t}{\sqrt{\pi}}\,\frac{I_n + I^*_{n+1}}{2}.$$

In addition to the above two methods, Brush's method and Daitche's first-order scheme are also implemented for comparison. Figure 1 shows the sedimentation velocity of a particle traveling until a dimensionless time of 50 when $\gamma = 1/2 < 5/8$ with a uniform time step of 0.01. The analytic solution is calculated and shown by the thick purple line. The numerical results from different methods are

differentiated by colors: FD Hybrid (red), PC method (green), Brush's method (blue) and Daitche's first-order scheme (yellow).

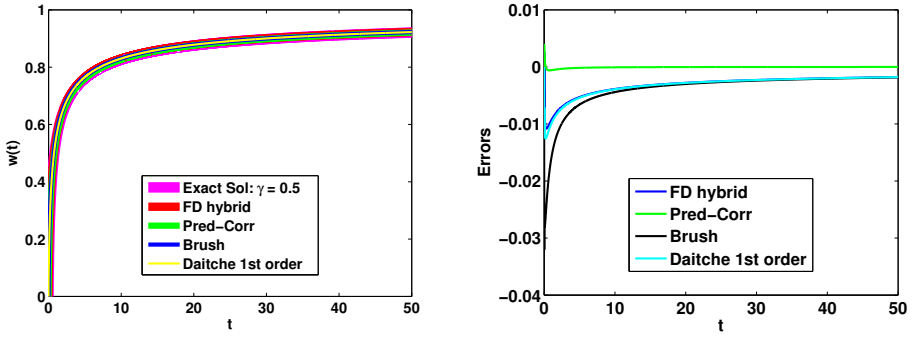

(a) $W(t), t \in (0, 50)$ (b) Error Plot

Figure 1: 1-D Sedimentation at $\gamma = 0.5$ via FD Hybrid, PC, Brush and Daitche's first-order methods.

As seen in Figure 1a, the numerical results all agree with the exact solution. The particle is released from rest, then accelerates until it reaches at a terminal velocity. The curves overlap with one another, making it difficult to differentiate among them. The error plot in Figure 1b helps highlight their differences. Here, the error is defined as the difference between the exact and numerical solutions. Among the four methods, PC is distinguished by having errors that are smaller from the beginning and later become closest to zero, while Brush's method strays farthest away from the exact solution at the very beginning. Both FD Hybrid and Daitche's first-order start off with smaller errors than Brush's; however, for long enough times, all three seem to agree with each other, which suggests that the FD Hybrid method is of first-order accuracy. We also observe that the FD Hybrid, Brush and Daitche's methods always underestimate the solution, for their errors stay negative for all time.

In addition, we show the "integrated error", i.e., the integral of the magnitude of the instantaneous error over the entire time interval in Table 1.

Table 1: Integrated Errors (Sedimentation)

Integrated Error	FD Hybrid	PC	Brush	Daitche
$\Delta t = 0.01$	0.15713	0.00336	0.19070	0.16053
$\Delta t = 0.001$	0.01555	0.00039	0.02453	0.01620

We calculate these for all four numerical methods when $\Delta t = 0.01$ and 0.001. It is not surprising that the integrated errors decrease as the time step gets finer for all cases. The PC method outperforms the other schemes.

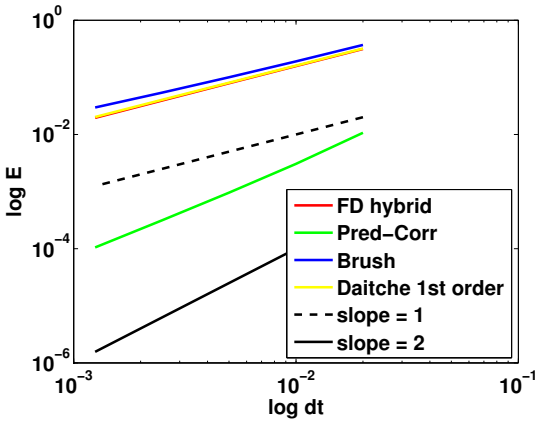

Figure 2: Log-Log plot of the integrated error versus Δt.

The Log-Log plot of the errors versus Δt shown in Figure 2 displays the order of accuracy clearly. The PC method is second-order accurate, while FD Hybrid, Daitche, and Brush are first order.

3.2. **Impulsive motion.** The second test problem models the case where the fluid is assumed to be at rest and the particle is given an initial velocity and allowed to relax freely in the viscous fluid, in the absence of gravity. The motion of the spherical particle is in one direction (e.g., parallel to unit vector $\mathbf{i}$ in Cartesian coordinates) and buoyancy effects are neglected. As we shall see below, the initial naive formulation of this problem leads to unphysical results, although it is mathematically well-posed and can still be used for benchmarking of the numerical results. This unphysical result turns out to be due to the infinite acceleration that would be implied by the mismatch between the fluid and particle velocities at the initial instant. The resolution of this paradox, shown in the second formulation, involves replacing the initial velocity of the particle with an impulsive force that acts on it, causing it to attain the desired velocity over a very short (nearly zero) time span.

3.2.1. *Formulation I.* Substitute $\mathbf{u} = 0$ (for a quiescent fluid) into (1.1); the equation of motion then reads

$$\begin{gathered} m_p\dot{\mathbf{V}} = -\frac{m_f}{2}\dot{\mathbf{V}} - 6\pi\mu a\mathbf{V} - 6a^2\sqrt{\pi\mu\rho_f}\int_0^t \frac{\dot{\mathbf{V}}(\tau)}{\sqrt{t-\tau}}\,d\tau \\ \mathbf{V}(0) = v_o\,\mathbf{i}, \end{gathered} \tag{3.4}$$

where $\mathbf{V}$ is the velocity of the particle, and v_o is its initial velocity. Let $\mathbf{V}(t) = \mathbf{i}\,y(t)$, choose the velocity scale v_0 and the time scale $(m_p + m_f/2)/(6\pi\mu a)$ to render y and t dimensionless, substitute into (3.4) and rename the dimensionless variables y and t again for simplicity, to get

$$\begin{gathered} \dot{y} = -y - \beta\int_0^t \frac{\dot{y}(\tau)}{\sqrt{t-\tau}}d\tau \\ y(0) = 1. \end{gathered} \tag{3.5}$$

The dynamics are determined by a single dimensionless parameter

$$\beta = \sqrt{\frac{9\rho_f}{\pi(2\rho_p + \rho_f)}}$$

that solely depends on the particle and fluid densities and whose value ranges from 0 to $3/\sqrt{\pi}$, as the ratio ρ_f/ρ_p goes from zero to infinity.

Analytic solution: Laplace transforms lead to the analytic solution (see Section 5.1 for details)

$$y(t) = \sum_{i=1}^{2} A_i X_i \exp(X_i^2 t)\operatorname{Erfc}\big(-X_i\sqrt{t}\,\big). \tag{3.6}$$

Erfc is the complementary error function defined earlier. Coefficients A_i and arguments X_i are given by (5.1) and (5.2) in the appendix. They are defined in terms of the parameter $b = \beta\sqrt{\pi}/2$. To better understand this solution, let us examine its asymptotic behavior for both short and long times.

Short-time behavior (near 0^+): For each term in (3.6), the series expansion for small t looks like

$$\exp\big(X^2\,t\big)\operatorname{Erfc}\big(-X\,\sqrt{t}\,\big) = 1 + \frac{2X\sqrt{t}}{\sqrt{\pi}} + X^2 t + \frac{4X^3 t^{3/2}}{3\sqrt{\pi}} + \mathcal{O}\big(t^2\big). \tag{3.7}$$

Thus,

$$\begin{aligned} y(t) &= (A_1X_1 + A_2X_2) + \sqrt{t}\frac{2}{\sqrt{\pi}}\big(A_1X_1^2 + A_2X_2^2\big) \\ &\quad + t\big(A_1X_1^3 + A_2X_2^3\big) + t^{3/2}\frac{4}{3\sqrt{\pi}}\big(A_1X_1^4 + A_2X_2^4\big) + \mathcal{O}\big(t^2\big) \\ &= 1 - t + \mathcal{O}\big(t^{3/2}\big). \end{aligned}$$

Here, we have used the results $\sum_{i=1}^2 A_iX_i = 1$, $\sum_{i=1}^2 A_iX_i^2 = 0$, $\sum_{i=1}^2 A_iX_i^3 = -1$, $\sum_{i=1}^2 A_iX_i^4 = 2b$.

Long-time behavior (near ∞): The large-t series expansion of each term has the form

$$\exp\big(X^2t\big)\operatorname{Erfc}\big(-X\sqrt{t}\big) = \frac{1}{X}\Big(-\sqrt{\frac{1}{t\pi}} + \frac{1}{2\sqrt{\pi}X^2}t^{-3/2} + \mathcal{O}\big(t^{-5/2}\big)\Big). \tag{3.8}$$

As such,

$$\begin{aligned} y(t) &= -t^{-1/2}\sqrt{\frac{1}{\pi}}(A_1 + A_2) + t^{-3/2}\frac{1}{2\sqrt{\pi}}\Big(\frac{A_1}{X_1^2} + \frac{A_2}{X_2^2}\Big) + \mathcal{O}\big(t^{-5/2}\big) \\ &= 2b\sqrt{\frac{1}{\pi}}t^{-1/2} + \mathcal{O}\big(t^{-3/2}\big) \\ &= \frac{\beta}{\sqrt{t}} + \mathcal{O}\big(t^{-3/2}\big) \end{aligned}$$

since $A_1 + A_2 = -2b$.

The fact that the longtime asymptotic form of the particle velocity decays relatively slowly as $t^{-1/2}$ leads to an unphysical result. Namely, if we consider the particle displacement, which is the integral of velocity with respect to time, the resulting integral diverges, which suggests that the particle will travel an infinite distance! Therefore, while the above impulsive motion problem is mathematically

acceptable and useful for benchmarking the numerical methods, it does not correctly model the physics of particle motion. To resolve this paradoxical issue, we re-examine this problem below using a formulation that takes into account the force of the impulse delivered to the particle.

Relationship to the 1-D sedimentation: Before we introduce the second formulation of the impulsive motion example, let us point out the strong similarity between this problem and the previous 1-D sedimentation. Consider (3.1) and (3.5) and notice their resemblance. The two dimensionless groups are themselves related by: $\beta = \sqrt{B/\pi}$. If we rescale time by B in the sedimentation problem, i.e., $T = Bt$, let τ' denote the scaled dummy variable of time-integration, and further introduce a variable $w(t) = 1 - W(t)$, (3.1) becomes

$$\frac{dw}{dT} = -w - \sqrt{\frac{B}{\pi}} \int_0^T \frac{\dot{w}(\tau')}{\sqrt{T-\tau'}}\, d\tau'. \tag{3.9}$$

Equation (3.9) appears to be equivalent to (3.5). To confirm that they are mathematically the same, we also need to examine the initial conditions. Since $w(0) = 1 - w(0) = 1$, the initial condition on w turns out to be the same as $y(0) = 1$. As for the initial acceleration,

$$\frac{dw}{dT}\Big|_{t=0} = \frac{d(1-W(t))}{d(Bt)}\Big|_{t=0} = -\frac{1}{B}\frac{dW}{dt}\Big|_{t=0} = -1\,.$$

The initial accelerations are thus also consistent because

$$\dot{y}(0) = -y(0) - \beta \int_0^0 \frac{\dot{y}(\tau)}{\sqrt{t-\tau}} d\tau = -1\,.$$

We see that the two problems are actually equivalent to each other mathematically, which raises an interesting question. Given the unphysical result from the first impulsive motion formulation, does a similar issue affect the sedimentation problem? The above equivalency seems to lead to the conclusion that while in the sedimentation problem, the particle eventually does relax to its final constant Stokes settling velocity, if the distance that it would lag behind another particle that always settled at that terminal velocity were measured, that distance would diverge in time. In other words, in an infinite container, if one particle is settling at the Stokes settling velocity, and another one is released from rest as the first particle passes by, the second particle will lag behind and the distance between them would diverge as $t \to \infty$. Therefore, there is a somewhat unphysical aspect to the sedimentation problem with the history force as well. This subtle issue appears not to have been noticed previously.

Numerical results: In the exact solution for $y(t)$, it appears that β has a critical value at $2/\sqrt{\pi}$ (where the quantities under the square roots undergo changes of sign). However, Coimbra and Rangel [11] pointed out that the critical value is only of mathematical relevance and does not imply a change of physical character of the problem. For the numerical experiments, we set $\beta = 1/\sqrt{\pi}$ which means that the particle is four times as dense as the fluid. Once again, four numerical methods are implemented: FD Hybrid, PC, Brush and Daitche's first-order methods. The scaled velocities computed by each method are plotted in Figure 3.

The particle slows down substantially right after the impulsive start, then approaches the expected time dependence of its velocity, $\beta/\sqrt{t}$, asymptotically as time increases.

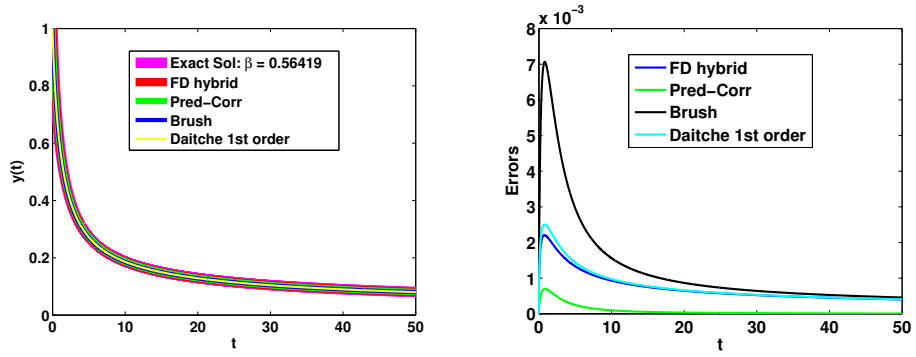

(a) $y(t), t \in (0, 50)$ (b) Error Plot

Figure 3: Impulsive Motion (Formulation I): FD vs. PC vs. Brush vs. Daitche's first-order method.

The PC method appears to yield the best result, as seen in Figure 3b which tracks the errors versus time. The other three methods differ at the beginning; however, given long enough time, their errors tend to approximately the same level. The integrated errors are displayed in Table 2 for two choices of time step.

Table 2: Integrated Errors (Impulsive Motion: Formulation I)

Integrated Error	FD Hybrid	PC	Brush	Daitche
$\Delta t = 0.01$	0.03685	0.00418	0.06459	0.03863
$\Delta t = 0.001$	0.00330	0.00042	0.01207	0.00389

Besides accuracy, the execution time of a numerical method is another important metric to evaluate its performance. For this purpose, we record the total computational time for each method and use the lowest one (FD Hybrid) as the unit of measurement. We find that the FD Hybrid and Brush's method both take approximately one time unit to run, while it takes the PC method about 1.5 times as long, and Daitche's method requires almost 6 time units.

Both of the proposed methods appear to work as they produce results that agree with the analytic solutions. On the merits of accuracy alone, the PC Method has an obvious edge. As for computational cost, FD Hybrid seems to be a little better. However, if the overall execution time is not prohibitively long, one can sacrifice the computation cost to achieve the better accuracy.

3.2.2. *Formulation II.* In [18], it is assumed that the initial velocities of the particle and the fluid are the same. But in the impulsive motion problem, while the fluid is at rest, the particle is given an initial velocity $v_0 \neq 0$, which suggests that a direct application of Maxey & Riley's equation might not be appropriate. As an alternative formulation, we can imagine that the particle and fluid both start from

rest, but that in addition to the Stokes drag and the history force, an impulsive force of the form $S\,\delta(t-0^+)$ should be included in the right-hand side of the equation of motion. The value 0^+ in the argument of the delta function suggests that the instantaneous impulse is applied ever so slightly after $t=0$. This avoids potential confusion in applying the initial condition. In this form, the initial velocity of the particle coincides with that of the fluid, so that we will be able to apply Maxey & Riley's equation to get

$$\begin{gathered}(m_p+\frac{m_f}{2})\,\dot{y} = -6\pi\mu a\, y - 6a^2\sqrt{\pi\mu\rho_f}\int_0^t \frac{\dot{y}(\tau)}{\sqrt{t-\tau}}d\tau + S\,\delta(t-0^+),\\ y(0)=0.\end{gathered} \tag{3.10}$$

Using the same time scale as before, $(m_p+m_f/2)/6\pi\mu a$, and the new velocity scale $S/(m_p+m_f/2)$, we obtain the dimensionless equation of motion

$$\begin{gathered}\dot{y} = -y - \beta\int_0^t \frac{\dot{y}(\tau)}{\sqrt{t-\tau}}d\tau + \delta(t-0^+),\\ y(0)=0.\end{gathered} \tag{3.11}$$

It should be noted that a delta function $\delta(t)$ has dimensions of the reciprocal of its argument, in this case time. If time is scaled like $t=T\hat{t}$, we have that $\delta(T\hat{t}) = (1/|T|)\delta(\hat{t})$.

Analytic solution: Using the Laplace transform, we can solve (3.11) analytically:

$$y(t) = \sum_{i=\pm} B_i X_i \exp(X_i^2 t)\mathrm{Erfc}(-X_i\sqrt{t}) \tag{3.12}$$

with the coefficients B_i and factors X_i given in (5.4) in Section 5.2. A similar asymptotic analysis can be performed to find the form of $y(t)$ when t is close to zero and when it approaches infinity, respectively.

Short-time behavior (near 0^+): Using (3.7), when $t\to 0^+$

$$\begin{aligned}y(t) &= \sum_{i=\pm} B_i X_i + t^{1/2}\frac{2}{\sqrt{\pi}}\sum_{i=\pm} B_i X_i^2 + t\sum_{i=\pm} B_i X_i^3 + t^{3/2}\frac{4}{3\sqrt{\pi}}\sum_{i=\pm} B_i X_i^4 + \mathcal{O}(t^2)\\ &= 1 - 2\beta\sqrt{t} + \mathcal{O}(t).\end{aligned}$$

Here we have used $\sum_{i=\pm} B_i X_i = 1$, $\sum_{i=\pm} B_i X_i^2 = -2b$, $\sum_{i=\pm} B_i X_i^3 = -1+4b^2$.

Long-time behavior (near ∞): By (3.8), when $t\to\infty$

$$\begin{aligned}y(t) &= -(B_+ + B_-)\sqrt{\frac{1}{t\pi}} + \Big(\frac{B_+}{X_+^2} + \frac{B_-}{X_-^2}\Big)\cdot\frac{1}{2\sqrt{\pi}}\cdot t^{-3/2} + \mathcal{O}\big(t^{-5/2}\big)\\ &= \frac{\beta}{2}t^{-3/2} + \mathcal{O}\big(t^{-5/2}\big).\end{aligned}$$

Note that $B_+ + B_- = 0$, $B_+/X_+^2 + B_-/X_-^2 = \beta\sqrt{\pi}$.

Displacement: With the long-time form of the velocity now decaying in time like $t^{-3/2}$, its integral with respect to time as the upper limit tends to infinity yields a finite value. Thus the unphysical result associated with the previous formulation does not plague this formulation of the impulsive start problem. For the purpose of numerical validation, both formulations can be used since they are mathematically well-posed problems. But the latter formulation is the correct physical one for the impulsive start example.

Numerical results: Because of the presence of the Dirac delta function $\delta(t-0^+)$, the above-mentioned numerical methods cannot be applied directly until a scheme for dealing with the delta function numerically has been devised. In order to make the system more amenable to a numerical approach, first express the solution in the form $y(t) = \alpha H(t-0^+) + w(t)$ where $H(t)$ is the Heaviside step function, defined by $H(t) = \int_{-\infty}^{t} \delta(s)\, ds$. The derivative of the solution is thus $\dot{y}(t) = \alpha\delta(t-0^+) + \dot{w}(t)$. Substitute this into (3.11) and balance the Delta functions on both sides of the equation by setting $\alpha = 1$ to get, for $t > 0^+$,

$$\dot{w}(t) = -1 - w(t) - \frac{\beta}{\sqrt{t}} - \beta \int_0^t \frac{\dot{w}(\tau)}{\sqrt{t-\tau}}\, d\tau\,. \tag{3.13}$$

The initial condition $y(0) = 0$ (applied at $t = 0 < 0^+$) implies that $w(0) = 0$. This provides an explanation for the appearance of the terms $(v_i - u_i)/\sqrt{t}$ as part of the history force in [20] and $w_i(0^+)/\sqrt{t}$ in [28]. However, there is a new term in the equation with singularity at $t = 0$. We choose the predictor-corrector (PC) method to treat this problem because we can modify it to evaluate the function at the midpoint of a time step so that it avoids the initial singularity. Specifically, when the scheme is applied to $\dot{y} = f(y,t) + r(t)$ where $r(t)$ has an explicit form in t (in our case, $r(t) = -\beta/\sqrt{t}$), we modify the PC method to

$$y^* = y_n + \Delta t\big[f^n + r^{n+\frac{1}{2}}\big]$$
$$y^{n+1} = y_n + \Delta t\big[\frac{f^n + f^*}{2} + r^{n+\frac{1}{2}}\big]$$

where $f^n = f(y_n, t_n)$, $f^* = f(y^*, t_n)$.

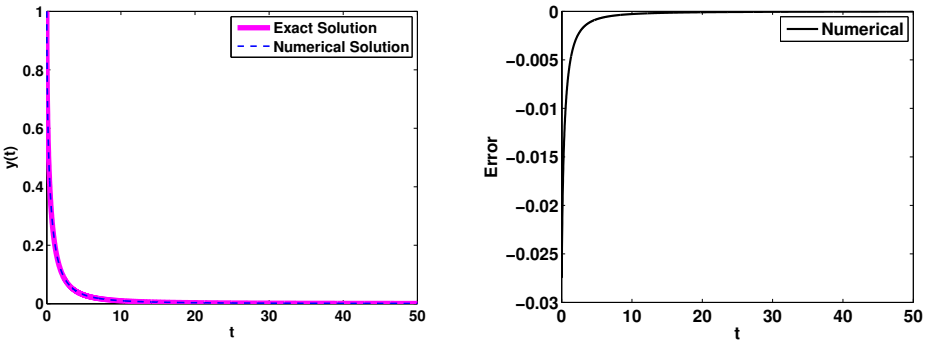

(a) Exact vs. Numerical (midPC) (b) Errors

Figure 4: Exact and numerical solutions $y(t)$ and the corresponding error.

The numerical results obtained with a time step of 0.01 are shown in Figure 4. The plot is obtained by solving (3.13) numerically to obtain $w(t)$ and calculating the resulting $y(t)$ from the relation $y(t) = 1 + w(t)$ for $t > 0$. The error is largest at the very beginning as illustrated in Figure 4b, which makes sense since the abrupt change (due to the impulsive force) occurs when $t = 0$. The integrated error in

this case is 0.0273, and as the time step is reduced to 0.001, the integrated error decreases to 0.0097, roughly decreasing by a factor of $\sqrt{10}$.

3.3. **Oscillatory Sliding Motion.** Here we introduce another physical problem for which a more interesting analytical solution can be obtained. Imagine that a spherical particle of mass m_p is placed in a cartridge filled with fluid which moves in a horizontal sliding oscillation, in the absence of gravity (i.e., without any sedimentation). The cartridge displacement is described by $\Delta\sin(\omega t)\mathbf{i}$, where ω is the temporal frequency of the linear oscillations and Δ denotes the amplitude. We expect that the particle will eventually also undergo a back and forth motion like its container, though not necessarily of the same amplitude or in phase with the cartridge. We take the particle to have the same initial velocity and acceleration as the fluid. Applying these to (1.1) and nondimensionalizing the system using time scale $1/\omega$ and length scale Δ result in the following dimensionless equation of motion:

$$\begin{gathered}\ddot{X}(t) = -\beta\dot{X}(t) + (1-\alpha)\sin t - \gamma\int_0^t \frac{\ddot{X}(\tau)}{\sqrt{t-\tau}}\,d\tau,\\ X(0) = 0, \quad \dot{X}(0) = 0.\end{gathered} \tag{3.14}$$

$X(t)$ is the particle's displacement relative to the fluid (i.e., in a frame of reference moving with the cartridge) and the three dimensionless groups appearing in this equation are are defined as follows:

$$\alpha = \frac{3m_f}{2m_p + m_f}, \quad \beta = \frac{6\pi\mu a}{\omega(m_p + m_f/2)}, \quad \gamma = \frac{6a^2\sqrt{\pi\mu\rho_f/\omega}}{m_p + m_f/2}.$$

Parameter α depends solely on the two densities, that is, $\alpha = 3\rho_f/(2\rho_p + \rho_f)$, and its value ranges from 0 to 3, from extremely dense particles relative to the fluid to particles (or bubbles) with very small densities; $\alpha = 1$ corresponds to neutrally buoyant particles. The second dimensionless group is the reciprocal of the Stokes number, i.e., $\beta = \mathrm{St}^{-1}$, which is a common parameter to characterize the behavior of particles suspended in a fluid flow. It represents the ratio of the relaxation time of the particle to the characteristic time of the flow: the bigger the Stokes number, the longer it takes a particle to relax to the same velocity as the fluid. The third parameter γ quantifies the importance of the history force. (Note that β in this section is different from the one defined earlier.)

Analytic solution: Once again Laplace transforms give the analytical solution (details are given in Section 5.3); namely,

$$X(t) = (1-\alpha)\Big(\sum_{i=1}^{6} A_i R_i \exp(R_i^2 t)\mathrm{Erfc}(-R_i\sqrt{t}) + A_7\Big), \tag{3.15}$$

where

$$R_1 = \exp\Big(\frac{\pi}{4}i\Big), \quad R_2 = \exp\Big(\frac{3\pi}{4}i\Big), \quad R_3 = \exp\Big(\frac{5\pi}{4}i\Big),$$
$$R_4 = \exp\Big(\frac{7\pi}{4}i\Big), \quad R_{5,6} = \frac{-\gamma\sqrt{\pi} \pm \sqrt{\gamma^2\pi - 4\beta}}{2}, \quad R_{7,8} = 0.$$

along with the coefficients

$$A_i = \frac{1}{R_i^2\prod_{j=1,j\neq i}^{j=6}(R_i - R_j)} \quad (i = 1, 2, \ldots, 6), \quad A_7 = \frac{1}{\beta}, \quad A_8 = \sum_{i=1}^{6}\frac{1}{R_i} \Big/ \prod_{i=1}^{6} R_i.$$

Numerical results: FD Hybrid, PC, Brush's and Daitche's first-order methods are tested and compared with the analytic solution. The parameters are set to $\alpha = 0.3571$, $\beta = 0.31$ and $\gamma = 0.3252$. The trajectories of the particle are traced until a time of 50, or roughly 8 periods of oscillation of the container.

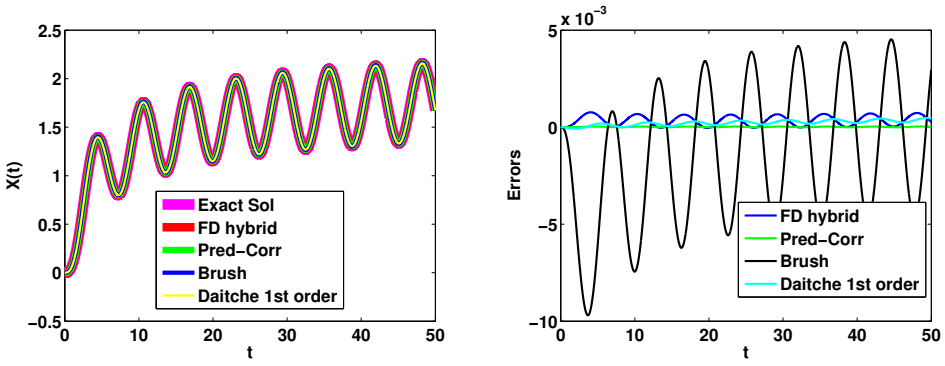

(a) $X(t), t \in (0, 50)$ (b) Error Plot

Figure 5: Oscillatory Sliding Motion: FD vs. PC vs. Brush vs. Daitche's first-order

As shown in Figure 5, all results agree and suggest that the particle is initially "thrown" forward from its original position by the starting motion of the container, but that after a while it stabilizes and oscillates about a new equilibrium position. It is not surprising that the errors oscillate as well as shown in Figure 5b. From the error plot, Brush's method presents the largest errors, while FD Hybrid and Daitche's method are of comparable magnitudes. The PC method produces the smallest errors. This can be seen more clearly in Table 3 which records the integrated errors when the time step is 0.01 and 0.001 respectively.

Table 3: Integrated Errors (Oscillatory Sliding Motion)

Integrated Error	FD Hybrid	PC	Brush	Daitche
$\Delta t = 0.01$	0.01740	0.00076	0.16238	0.01132
$\Delta t = 0.001$	0.00375	2.33314e-05	0.05156	0.00015

4. Conclusions

Two methods were introduced to approximate history integrals of the form $\int_0^t f(\tau)/\sqrt{t-\tau}\,d\tau$ and $\int_0^t \dot{f}(\tau)/\sqrt{t-\tau}\,d\tau$ numerically. For the former integral, trapezoidal rule together with a forward difference approximation of the derivative of f (after integration-by-parts) led to the FD Hybrid method; for the latter, the derivative $\dot{f}$ was treated by central differences at the mid-points of the time

intervals, leading to an approximation that could be used effectively in conjunction with the Predictor-Corrector (PC) method to integrate the equations of motion for particles affected by the history force. Both were applied to three one-dimensional test problems that describe the physical problems of sedimentation, impulsive motion and oscillatory sliding motion of a particle in a fluid. The numerical results were compared with analytic solutions obtained by Laplace transforms and both methods were shown to work well in all cases. We quantified their performance in terms of accuracy and computation time, while comparing them to Brush's and Daitche's first-order methods from the existing literature.

In all three cases, the PC method performed best, showing advantages in the following respects: (i) the update expression is straightforward, making it easy to implement; (ii) on the three one-dimensional problems tested, PC is the most accurate; (iii) although it is not the fastest method, compared to the faster FD Hybrid and Brush's methods, its computational time is within an acceptable range; (iv) in the second formulation of the impulsive motion problem, it has the advantage that it avoids having to evaluate the forcing function at its point of singularity. Having validated these numerical schemes, they can be applied with some confidence to more complex problems for which analytic solutions are not available [29].

The test problems that we considered are useful for benchmarking the numerical methods in that their exact solutions could be obtained by Laplace transforms. Our solution for the oscillatory sliding motion is new. For the impulsive start problem, we provided two formulations, pointing out that the solution that results by assuming that the particle has a different initial velocity than the fluid, while mathematically acceptable, is not physically correct. This pointed out a subtle issue with the interpretation of the existing solution to the sedimentation problem as well, since it maps directly onto the first formulation of the impulsive start example. The resolution of the unphysical behavior involved introducing an impulsive force as a forcing in the equation, while allowing the initial velocities of the particle and the fluid to be the same.

5. Appendix: Analytical solutions

We now provide the details for obtaining the exact solution for both formulations of the impulsive motion example and the oscillating sliding motion problem analytically by use of Laplace transform.

5.1. **Impulsive motion: formulation I.** Apply Laplace transform to (3.5) and let s denote the Laplace transform variable. The Laplace transform of $y(t)$ is denoted by $Y(s)$ and is found to be

$$Y(s) = \frac{\sqrt{s} + \beta\sqrt{\pi}}{s\sqrt{s} + \beta\sqrt{\pi}s + \sqrt{s}}.$$

The denominator is a cubic polynomial in $\sqrt{s}$ with the three roots:

$$X_0 = 0, \quad X_1 = -b + \sqrt{b^2 - 1}, \quad X_2 = -b - \sqrt{b^2 - 1}\,, \tag{5.1}$$

where $b = \beta\sqrt{\pi}/2$. $Y(s)$ can then be written as a partial fraction expansion of the form

$$Y(s) = \sum_{i=0}^{2} \frac{A_i}{\sqrt{s} - X_i}$$

in which the coefficients are given by

$$A_0 = 2b, \quad A_1 = \frac{1 - 2b^2 - 2b\sqrt{b^2-1}}{2\sqrt{b^2-1}}, \quad A_2 = \frac{2b^2 - 1 - 2b\sqrt{b^2-1}}{2\sqrt{b^2-1}}. \tag{5.2}$$

The inverse Laplace transform of $1/(\sqrt{s}-X_i)$ is $1/\sqrt{\pi t}+X_i \exp(X_i^2 t)\mathrm{Erfc}\left(-X_i\sqrt{t}\right)$. Noting that $A_0 + A_1 + A_2 = 0$, the analytical solution for the impulsive motion problem simplifies to

$$y(t) = \sum_{i=1}^{2} A_i X_i \exp(X_i^2 t)\mathrm{Erfc}\big(-X_i\sqrt{t}\,\big). \tag{5.3}$$

5.2. **Impulsive motion: formulation II.** Upon taking the Laplace transform of (3.11), we obtain

$$sY = -Y - \beta s Y\sqrt{\frac{\pi}{s}} + 1 \quad \Rightarrow \quad Y = \frac{1}{s + \beta\sqrt{\pi}\sqrt{s} + 1}.$$

There are two roots (in $\sqrt{s}$) for the denominator, and to differentiate them from the previous formulation, we denote them by X_+ & X_- with coefficients B_+ & B_- even though $X_{+(-)} \equiv X_{1(2)}$:

$$X_{+,-} = -b \pm \sqrt{b^2-1}, \quad B_{+,-} = \pm\frac{1}{2\sqrt{b^2-1}}. \tag{5.4}$$

The partial fraction expansion of $Y(s)$ then reads

$$Y(s) = \frac{B_+}{\sqrt{s} - X_+} + \frac{B_-}{\sqrt{s} - X_-},$$

whose inverse Laplace transform provides the exact solution given in (3.11).

5.3. **Oscillatory sliding motion.** Applying Laplace transform to (3.14),

$$s^2 X(s) = -\beta s X + \frac{1-\alpha}{s^2+1} - \gamma s^2 X\sqrt{\frac{\pi}{s}}\,,$$

where $X(s) = \mathcal{L}\{X(t)\}$. Solving for $X(s)$ we get

$$X(s) = \frac{1-\alpha}{(s^2+1)(s^2 + \gamma\sqrt{\pi}s\sqrt{s} + \beta s)}\,.$$

Let $R = \sqrt{s}$ and find the roots of $(R^4+1)(R^2 + \gamma\sqrt{\pi}R + \beta)R^2$. Denote these by R_i and the corresponding coefficients in the partial fraction expansion of $X(s)$ by A_i $(i = 1, \ldots, 8)$. They are given explicitly following (3.15). In terms of these, $X(s)$ can be written as

$$X(s) = (1-\alpha)\Big(\sum_{i=1}^{6} \frac{A_i}{\sqrt{s} - R_i} + A_7\frac{1}{s} + A_8\frac{1}{\sqrt{s}}\Big).$$

Noting that the inverse Laplace transform of $1/(\sqrt{s} - R_i)$ is

$$(1/\sqrt{\pi t} + R_i \exp(R_i^2 t)\mathrm{Erfc}(-R_i\sqrt{t})),$$

that of $1/\sqrt{s}$ is $1/\sqrt{\pi t}$, and that of $1/s$ is the Heaviside step function, the solution for $X(t)$ is given by

$$X(t) = (1-\alpha)\Big(\sum_{i=1}^{6} A_i\Big(\frac{1}{\sqrt{\pi t}} + R_i \exp(R_i^2 t)\mathrm{Erfc}(-R_i\sqrt{t})\Big) + A_7 H(t) + A_8\frac{1}{\sqrt{\pi t}}\Big).$$

Using the fact that $A_8 + \sum_{i=1}^{6} A_i = 0$, this simplifies for positive time to the result given in (3.15).

Acknowledgement. Shujing Xu thanks the Institute of Mathematical Sciences at Claremont Graduate University for the Director's Fellowship that partially supported her graduate studies.

References

[1] P. Alexander; High order computation of the history term in the equation of motion for a spherical particle in a fluid. J. Sci. Comput., 21(2):129–143, 2004.

[2] A. B. Basset; A treatise on hydrodynamics with numerous examples. Dover Publications Inc., New York, 1961.

[3] A. Belmonte, J. Jacobsen, A Jayaraman; Monotone solutions of a nonautonomous differential equation for a sedimenting sphere. Electronic Journal of Differential Equations, 2001(62):1–17, 2001.

[4] F. Bombardelli, A. González, Y. Niño; Computation of the particle Basset force with a fractional-derivative approach. Journal of Hydraulic Engineering, 134(10):1513–1520, 2008.

[5] J. V. Boussinesq; Sur la résistance qu'oppose un fluide indéfini au repos, sans pesanteur, au mouvement varié d'une sphère solide qu'il mouille sur toute sa surface, quand les vitesses restent bien continues et assez faibles pour que leurs carrés et produits soient négligeables. Comptes Rendu de l'Academie des Sciences, 100, 1885.

[6] L. M. Brush, H. W. Wo, B. C. Yen; Accelerated motion of a sphere in a viscous fluid. Journal of the Hydraulics Division, 90:149–160, 1964.

[7] F. Candelier, J. R. Angilella, M. Souhar; On the effect of the Boussinesq–Basset force on the radial migration of a Stokes particle in a vortex. Physics of Fluids, 16(5):1765–1776, 2004.

[8] E. J. Chang, M. R. Maxey; Unsteady flow about a sphere at low to moderate Reynolds number. part 1. oscillatory motion. Journal of Fluid Mechanics, 277:347–379, 9 1994.

[9] E. J. Chang, M. R. Maxey; Unsteady flow about a sphere at low to moderate Reynolds number. part 2. accelerated motion. Journal of Fluid Mechanics, 303:133–153, 10 1995.

[10] R. Clift, J. R. Grace, M. E. Weber; Bubbles, drops, and particles. Dover Publications, 2005.

[11] C. F. M. Coimbra and R. H. Rangel. General solution of the particle momentum equation in unsteady Stokes flows. J. Fluid Mech., 370:53–72, 1998.

[12] A. Daitche; Advection of inertial particles in the presence of the history force: Higher order numerical schemes. Technical Report arXiv:1210.2576, 2012.

[13] A. Daitche and T. Tél. Memory effects are relevant for chaotic advection of inertial particles. Phys. Rev. Lett., 107:244501, 2011.

[14] I. Kim, S. Elghobashi, W. A. Sirignano; On the equation for spherical-particle motion: effect of Reynolds and acceleration numbers. Journal of Fluid Mechanics, 367:221–253, 6 1998.

[15] Y. Ling, J. L. Wagner, S. J. Beresh, S. P. Kearney, and S. Balachandar; Interaction of a planar shock wave with a dense particle curtain: Modeling and experiments. Physics of Fluids, 24(11):113301, 2012

[16] P. M. Lovalenti and J. F. Brady; The hydrodynamic force on a rigid particle undergoing arbitrary time-dependent motion at small Reynolds number. Journal of Fluid Mechanics, 256:561–605, 1993.

[17] N. Lukerchenko; Basset history force for the bed load sediment transport. In Proceedings of the First IAHR European Division Congress, 4–6 May 2010, 2010.

[18] M. R. Maxey and J. J. Riley; Equation of motion for a small rigid sphere in a nonuniform flow. Physics of Fluids, 26(4):883–889, 1983.

[19] R. Mei, R. J. Adrian, T. J. Hanratty; Particle dispersion in isotropic turbulence under Stokes drag and Basset force with gravitational settling. Journal of Fluid Mechanics, 225:481–495, 1991.

[20] E. E. Michaelides; A novel way of computing the Basset term in unsteady multiphase flow computations. Physics of Fluids A: Fluid Dynamics, 4(7):1579–1582, 1992.

[21] E. E. Michaelides; Review - the transient equation of motion for particles, bubbles, and droplets. Journal of Fluids Engineering, 119(2):233+, 1997.

[22] Y. A. Nevskii, A. N. Osiptsov; The effect of unsteady and history forces in the gravity convection of suspensions. Moscow University Mechanics Bulletin, 63:85–88, 2008.

[23] M. W. Reeks, S. McKee; The dispersive effects of Basset history forces on particle motion in a turbulent flow. Physics of Fluids, 27(7):1573–1582, 1984.
[24] M. A. T. van Hinsberg, J. H. M. ten Thije Boonkkamp, H. J. H. Clercx; An efficient, second order method for the approximation of the Basset history force. J. Comput. Physics, 230:1465-1478, 2011.
[25] E. V. Visitskii, A. G. Petrov; Structurization of solid particles in a liquid medium under the action of a standing ultrasonic wave field. Doklady Physics, 51:328–333, 2006.
[26] Y. V. Visitskii, A. G. Petrov, M. M. Shunderyuk; The motion of a particle in a viscous fluid under gravity, vibration and Basset's force. Journal of Applied Mathematics and Mechanics, 73(5):548 – 557, 2009.
[27] I. S. Vodop'yanov, A. G. Petrov, M. M. Shunderyuk; Unsteady sedimentation of a spherical solid particle in a viscous fluid. Fluid Dynamics, 45:254–263, 2010.
[28] D. J. Vojir, E. E. Michaelides; Effect of the history term on the motion of rigid spheres in a viscous fluid. International Journal of Multiphase Flow, 20(3):547 – 556, 1994.
[29] S. Xu; Effects of History and Lift Forces on Particle Trajectories in Oscillatory Rotating Fluids. PhD thesis, Claremont Graduate University, August 2014.
[30] S. M. Yang, L. G. Leal; A note on memory-integral contributions to the force on an accelerating spherical drop at low Reynolds number. Physics of Fluids A: Fluid Dynamics, 3(7):1822–1824, 1991.
[31] C. S. Yih; Fluid Mechanics: A Concise Introduction to the Theory. West River Press, 1977.

Shujing Xu
Institute of Mathematical Sciences, Claremont Graduate University, Claremont, CA 91711, USA
E-mail address: flora.xushujing@gmail.com

Ali Nadim
Institute of Mathematical Sciences, Claremont Graduate University, Claremont, CA 91711, USA
E-mail address: ali.nadim@cgu.edu